Desalination and Water Treatment
www.deswater.com

doi: 10.1080/19443994.2015.1085915

57 (2016) 17523–17536
August

Taylor & Francis
Taylor & Francis Group

Synthesis of chitosan based semi-IPN hydrogels using epichlorohydrine as crosslinker to study the adsorption kinetics of Rhodamine B

Fahad S. Al-Mubaddel[a], Muhammad Omer Aijaz[a,b], Sajjad Haider[a,*], Adnan Haider[c], Waheed A. Almasry[a], Ahmed Sadeq Al-Fatesh[a]

[a]*Department of Chemical Engineering, College of Engineering, King Saud University, P.O. Box 800, Riyadh 11421, Saudi Arabia, emails: energykingdom@hotmail.com (F.S. Al-Mubaddel), omeraijaz599@gmail.com (M.O. Aijaz), Tel. +966 1 4675579; emails: shaider@ksu.edu.sa (S. Haider), Walmasry@ksu.edu.sa (W.A. Almasry), aalfatesh@ksu.edu.sa (A.S. Al-Fatesh)*

[b]*Center of Excellence for Research in Engineering Materials (CEREM), Advanced Manufacturing Institute, King Saud University, P.O. Box 800, Riyadh 11421, Saudi Arabia*

[c]*Department of Polymer Science and Engineering, School of Applied Chemical Engineering, Kyungpook National University, Daegu 702-701, Republic of Korea, email: adnan_afridi9294@yahoo.com*

Received 3 February 2015; Accepted 15 August 2015

ABSTRACT

The present study is focused on the preparation of chitosan (CS)/polyacrylonitrile (PAN) blend and semi-interpenetrating polymer network (sIPN) hydrogel films, and their application to the adsorption of Rhodamine B dye. The CS/PAN blend hydrogel films were prepared by solution casting technique. To prepare sIPN, CS was cross-linked with epichlorohydrin (ECH). The developed CS/PAN blends and sIPN hydrogels were characterized with field emission scanning electron microscope (FESEM) and Fourier transform infrared (FT-IR) spectroscope. The FESEM micrographs showed no phase separation between CS and PAN. The cross-linking of CS in the sIPN was confirmed by FT-IR. The degree of swelling, W_{UB} water content, and aqueous stabilities of the blends and sIPN hydrogels were examined at room temperature. Blend film (C8/P2) showed highest % degree of swelling (~2,400%), increased % unbound water (W_{UB}) (52%), and fair degree of aqueous stability. The swelling of the blends decreased not only with an increase in PAN content but also with cross-linking. At the same CS and PAN composition (C8/P2), sIPN hydrogel exhibited a relatively low degree of swelling (~245%), W_{UB}, and a high degree of aqueous stability. The potential of the optimized hydrogel film as an adsorbent was evaluated. The q_{max} value for c-sIPN was much higher compared to C8/P2 blend film. The adsorption kinetics of Rhodamine B (RB) was observed to follow pseudo-second-order equation and the equilibrium adsorption obeyed Langmuir isotherm equation. The kinetics and adsorption isotherm indicated that the mechanism of adsorption is chemical. However, the FTIR spectra after adsorption showed hydrogen bonding.

Keywords: Chitosan; Polyacrylonitrile; sIPN; Hydrogels; Dye; Adsorption; Mechanism

*Corresponding author.

1. Introduction

Hydrogels are hydrophilic three-dimensional superabsorbant polymer networks (cross-linked either physically or chemically), which retain water (thousand times of their dry weight) within their structure without dissolution. Due to this ability and the inherent biocompatibility and low toxicity, recently researchers are paying more attention to hydrogel for potential applications in environmental and biomedical fields [1–3]. Hydrogels have also shown reversible transformation (swelling and shrinking) upon exposure to stimuli (such as temperature, pH, solvent composition, ionic strength, magnetic, electric fields). The stimuli-sensitive hydrogels have potential applications as an artificial muscle, controlled drug delivery systems, soft actuators, and separation membranes, and will be of a great importance for switches, chemical valves, and electromechanical engines [4–7]. According to the European disposables and nonwovens association, the production of the superabsorbent polymer resins was more than one million tons in the late 1990s [8,9], which increased to 1,483,000 tons (623,000 tons in Asia, 490,000 tons in North America, and 370,000 tons in Europe) in 2005 [9,10]. Regardless of these advantages, researchers are still faced with problems (such as low mechanical strength, degradation on exposure to environment, difficulty in handing and loading) in using these materials for advance applications. To solve these problems, more research on the development and reporting of hydrogel is needed [11–13]. A variety of synthetic (e.g. polyethylene glycol (PEG), polyvinyl alcohol (PVA), polyhydroxyethylmethacrylate (PHEMA), poly(acrylic acid) (PAA), polymethyl acrylate (PMA), and polyacrylamide (PAM) [8], polyacrylamide (PAAm), polyacrylic acid (PAA), poly(acrylamide-co-itaconic acid) (PAAmIA), poly(acrylic acid-co-itaconic acid) (PAAIA) [14], poly(acrylamide-co-crotonic acid) (PAAmCA), poly (acrylic acid-co-crotonic acid) (PAACA), PAA, PAAm [15]), and natural materials (e.g. polysaccharides, cellulose, proteins) have been used to synthesize hydrogel [8,16]. These combinations of the natural and synthetic polymers have shown fruitful results. However, in some cases, the fast degradation rate and weak strength of the hydrogel are not improved significantly under wet environments. Hence, to reduce their fast degradation and make them stable in aqueous environment, another simple and feasible technique known as semi-interpenetrating polymer network (sIPN) has been used to produce sIPN hydrogel [17]. The sIPN is a crucial class of hydrogels. It is a combination of two or more polymers in which one polymer is converted into a network via cross-linking and the other remains in the linear form. The sIPN structures have been reported by various research groups [18–20] as a new solution to overcome the major disadvantages of hydrogels (i.e. their relatively low strength and degradation in the wet environment) [21].

The removal of dyes using various adsorbents has been extensively studied and reported in the literature [22–25]. Polymers with different functional groups have shown great potential as adsorbents in the environmental applications. Polymer hydrogels with different functional groups (such as amino, hydroxyl, carboxyl, imidazole, and hydrazine groups [26]) have recently been more focused. Hydrogels such as polyvinylpirrolidone (PVP), PVP/methacrylic acid, PAM/PAA, chitosan, and its derivatives have been shown to make complexes with dyes and metal ions [27–29]. The main advantages of the use of hydrogel as adsorbents are easy loading, formation of chelation complex, prospect of semi-continuous operation, high swelling, and wettability [26,30]. The swelling and wettability will help in adsorption of the target molecules or ions since swelling is likely to provide more specific surface area and expose more functional groups for adsorption [26].

To further research on these models, the combination of the natural CS and synthetic PAN was studied. CS and its derivatives with synthetic polymers were investigated extensively. CS produced by alkaline N-deacetylation of chitin is the most facile chemical alteration and gives an useful derivative [31,32]. PAN is frequently used as an active component of ion-exchangers. PAN has the advantage of relatively easy modification of its physicochemical properties (e.g. hydrophilicity, porosity, mechanical strength). This unique property is imparted to PAN by its nitrile group. PAN forms hydrogen bonds and donor–acceptor complexes (chelation) with positively charged species [33].

In this study, we have focused on the preparation of CS/PAN blend and sIPN hydrogel systems to overcome the instability of CS hydrogel while keeping the swelling ratio as high as possible. The optimized hydrogel films were then used as adsorbents for the adsorption of RB dye from synthetic wastewaters. We believe that sIPN hydrogel films will prove a potential step forward in the use of these materials in various applications, particularly in protecting the aqueous environment.

2. Material and methods

2.1. Materials

Medium molecular weight (M_w) CS powder $(C_8H_{13}NO_5)_n$, average M_W 150,000 PAN $(C_3H_3N)_n$,

acetic acid (($C_2H_4O_2$) AcOH), dimethyl sulfoxide ((C_2H_6OS), DMSO), ethanol ((C_2H_5OH) ETOH) absolute, and sodium hydroxide (NaOH) were purchased from Sigma-Aldrich, Alfa Aesar, Paneac Quimica SAU, and Scharlab S.L., respectively. Epichlorohydrin (($C_3H_5C_lO$) ECH) was purchased from Loba Chemie. RB dye was purchased from Sigma-Aldrich. All the chemicals were of analytical grade and were used without further purification. Distilled water was used for the preparation of solutions and the measurement of swelling and stability.

2.2. Preparation of CS/PAN blend films

2 wt.% CS solution was prepared by dissolving CS in a 2 wt.% AcOH solution and distilled water via a sonicator bath (Branson Model 2510) at 45°C for 90 min. After dissolution, the solution was stirred for 15 min using magnetic stirrers (Model Cerastir 30539) and finally filtered through a mesh with 0.063 mm pore size to remove any undissolved particles and obtain homogeneous solution. 2 wt.% PAN solution was prepared by dissolving PAN in DMSO via a magnetic stirrer at room temperature (T_r) for 1 h. The solutions of CS and PAN were mixed homogenously at different ratios [34] (the sample name and code are given in Table 1) using a mechanical stirrer at a speed of 2,000 rotation per minute (rpm) for 15 h. The mixing was followed by 30 min sonication to remove the bubbles. The mixed solution was then poured into a petri dish and placed into an oven for drying at 40°C for 4 d. After drying in oven, the films were further dried in the vacuum oven at 60°C and −0.1 MPa until complete dryness. Dried films of CS/PAN were detached from the petri dish and stored into a closed plastic bag for characterization.

Table 1
Sample names and code details where C = CS and P = PAN

CS/PAN blend films				
Sample codes	C8/P2	C6/P4	C4/P6	C2/P8
Code details	C8 = 80[a]	C6 = 60[a]	C4 = 40[a]	C2 = 20[a]
	P2 = 20[a]	P4 = 40[a]	P6 = 60[a]	P8 = 80[a]
sIPN hydrogel films				
Sample codes	a-sIPN	b-sIPN	c-sIPN	d-sIPN
Code details	C8 = 80[a]	C8 = 80[a]	C8 = 80[a]	C8 = 80[a]
	P2 = 20[a]	P2 = 20[a]	P2 = 20[a]	P2 = 20[a]
	b = 0.01[b]	*c* = 0.02[b]	*d* = 0.03[b]	*e* = 0.04[b]

[a]Ratios of CS and PAN in wt.%.
[b]Indicates Mol/L^{-1} of ECH.

2.3. Preparation of sIPN hydrogel film

To prepare sIPN, CS in the CS/PAN (C8/P2) was cross-linked with ECH. Briefly, the CS hydrogel film was immersed in 10 mL of 0.01 mol L^{-1} ECH solution (prepared in NaOH solution 0.5 mol L^{-1}) at 40°C under continuous agitation for 180 min. When the reaction is complete, the sample was taken out of the container, washed with distilled water, dried at room temperature, and stored. The same method was repeated with different concentrations (0.01–0.04 mol L^{-1}) of ECH. The samples' names and codes are described in Table 1.

2.4. Morphology study

The non-freezed surface morphologies, and the freeze-dried surface, and cross section morphologies of the CS/PAN blend ((a) C8/P2, (b) C6/P4, (c) C4/P6, (d) C2/P8) films, and c-sIPN hydrogel film were studied using FESEM (FEI Quanta 200 (FE SEM-2)). CS/PAN, sIPN, and freeze-dried films were fixed onto a holder with the aid of a carbon tape and then placed in the sputtering machine for platinum coating to increase their electrical conductivity. After platinum coating, the samples were examined under high vacuum. The same method was repeated for examining the cross section of the fractured films.

2.5. FT-IR study

Infrared spectra of the CS powder, PAN powder, CS/PAN, and sIPN films were studied using Fourier transform infrared spectrometer (Bruker Vertex 70). The KBr disks of the samples were prepared by mixing and grounding the samples with KBr powder in a mortar with a pestle. The mixture was then shaped into disks under hydraulic press. The sample disks were placed into FTIR and spectral measurements were recorded in the wave number range of 400–4,000 cm^{-1}. The data were processed by OPUS 6.0 (Bruker) Software, which was baseline corrected by rubber band method with CO_2 and H_2O bands excluded.

2.6. Degree of swelling

For the measurement of the % degree of swelling, the CS/PAN and sIPN films were thoroughly dried under vacuum at 60°C and −0.1 MPa until a constant weight was achieved. Each sample was then weighed and the weight is recorded as dry weight. The dried samples were separately immersed in vials containing 15 mL of distilled water (with pH 6.8) at room

temperature. Each sample was taken out of the vial at regular intervals (5–2,880 min), wiped between two filter papers to remove the excess surface water and then weighed. This weight is recorded as swollen weight. The degree of swelling was calculated with Eq. (1):

$$\text{Swelling ratio } (\%) = \left(\frac{W_S - W_D}{W_D}\right) \times 100 \quad (1)$$

where W_S and W_D are the weights of the swollen and dried samples, respectively.

2.7. Stability study

The % degree of stability of the CS/PAN and sIPN films was measured by thoroughly drying the samples under vacuum at 60°C and −0.1 MPa until constant weights were achieved. The dried samples were weighed and the observations were recorded on the data sheet as initial weight. After weighting, the samples were separately dipped into distilled water (with pH 6.8) in a vial container. The samples were allowed to remain in the distilled water at room temperature for different time intervals (i.e. 8, 24, 48, 72, and 96 h). The samples were taken out of the vial at the mentioned time intervals, dried and weighed, and the observations were recorded on the data sheet as final weights. The % degree of stability was expressed by Eq. (2):

$$\text{Stability } (\%) = \left(\frac{W_2}{W_1}\right) \times 100 \quad (2)$$

where W_1 and W_2 are the initial and final weights of the dried hydrogel.

2.8. State of water study

The states of water in the CS/PAN blend and sIPN hydrogel films were measured by freeze dryer technique using CHRIST freeze dryer (Model; ALPHA1-2 LD Plus). Thoroughly dried samples were weighed and their weights were recorded as initial weights. The samples were then immersed in separated vials containing distilled water. The samples were allowed to swell until equilibrium. The swelled samples were taken out of the vials and their weights were measured. The samples were then placed in the freeze dryer shelves for freezing at −40°C for 20 min followed by drying at −40°C and 1.6 mbar for 60 min. To remove even the traces of unbounded water from the structure, the samples were further dried at −55°C and 0.04 mbar for 20 min. Finally, the samples were removed from the shelves and their weights were measured. The total amount of water (W_T) was calculated by subtracting the initial dry weight (W_I) from the swollen weight (W_S). The % amount of total (W_T), unbound water (W_{UB}) and bound water (W_B) were determined from Eqs. (3)–(5) [35]:

$$W_T\ (\%) = \left(\frac{W_S - W_I}{W_S}\right) \times 100 \quad (3)$$

where W_T, W_S, and W_I are the amounts of total, swollen, and initial weights of the sample, respectively.

$$W_B\ (\%) = \left(\frac{W_F - W_I}{W_S}\right) \times 100 \quad (4)$$

where W_F is the weight of freeze-dried sample. The amount of W_{UB} was determined by subtracting the amount of W_B from W_T:

$$W_{UB}\ (\%) = W_T\ (\%) - W_B\ (\%) \quad (5)$$

2.9. Adsorption study

Dried samples of the CS/PAN and sIPN films were added separately to 10 mL synthetic solutions of RB dye (100 ppm) and agitated (in a shaker bath) by a batch technique as a function of time until 600 min at 25°C and at pH 7. Equilibrium time was determined from the saturation point of the adsorption kinetics data. Adsorption equilibrium isotherm was also studied as a function of the concentration of dye at 25°C. The concentrations of RB dye in solution after adsorption were determined with UV/vis spectrometer (Labomed; Model UVD-2950). The amount adsorbed was calculated using Eq. (6):

$$q = \frac{(C_0 - C_f)V}{M} \quad (6)$$

where q is the amount adsorbed (mg g^{-1}), C_0 and C_f are the initial and final concentrations (mg L^{-1}) of the dye, respectively. V is the solution volume (L) and M is the amount of adsorbent (g) used.

3. Results and discussion

3.1. Blend and hydrogel film morphology

Fig. 1 shows the surface and cross-sectional FESEM micrographs of the CS/PAN blend and sIPN films.

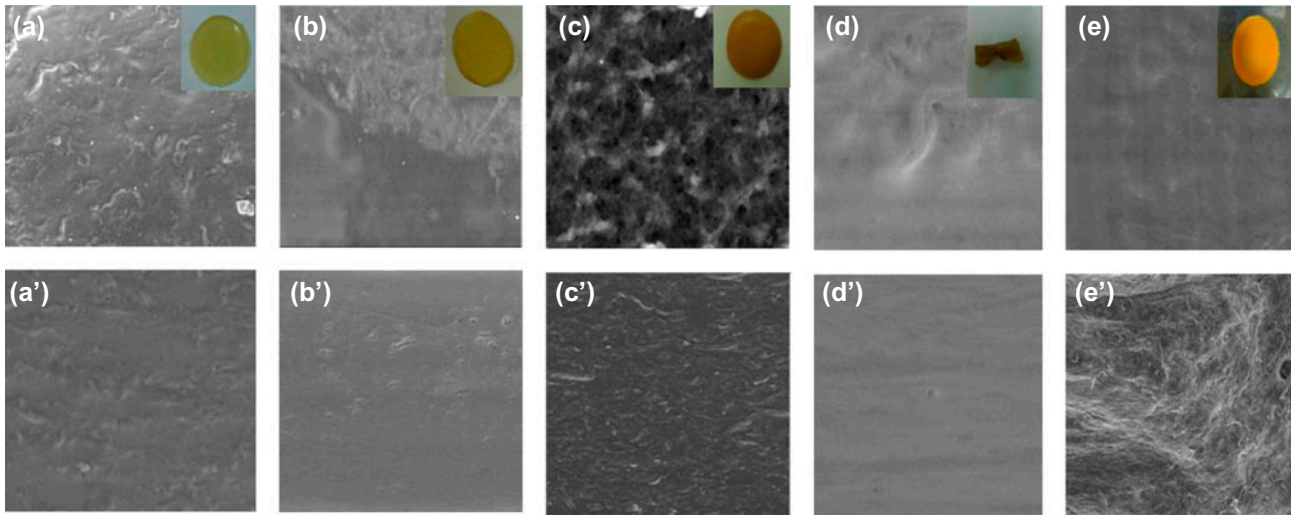

Fig. 1. FESEM micrographs of the surface CS/PAN hydrogels: (a) C8/P2, (b) C6/P4, (c) C4/P6, (d) C2/P8, and (e) c-sIPN; and cross section: (a′) C8/P2, (b′) C6/P4, (c′) C4/P6, (d′) C2/P8, and (e′) c-sIPN.

The FESEM micrographs and the digital images (shown in the inset of the FE SEM micrographs) of the surface of the blends (Fig. 1(a)–(d)) and sIPN (Fig. 1(e)) indicated good miscibility and no visible phase separation between CS and PAN. All the films were homogenous. The miscibility was attributed to the hydrogen bonding interactions between the various functional groups present in the two polymers [36,37]. Similar to the surface morphologies, the cross-sectional morphologies of the blends (Fig. 1(a′)–(d′)) and sIPN (Fig. 1(e′)) showed no phase separation behavior. This homogenous texture of the films confirmed our hypothesis that both solutions of CS and PAN in the mixture were homogenized from top to bottom. Besides miscibility, the effect of cross-linking on the morphology of sIPN was also studied. The FESEM micrographs showed homogenous surface as well as cross-sectional morphologies for the sIPN (Fig. 1(e) and (e′)) films. This further suggested that both the polymers are miscible and cross-linking did not affect this miscibility.

3.2. FTIR study

Fig. 2(I) shows the FTIR spectra of the CS, PAN, and CS/PAN blends. The spectra of CS show (Fig. 2I (a)) the characteristic bands of $-NH_2$ and –OH stretching vibrations in the range of 3,500–3,450 cm^{-1}, and amide I and amide III bands in the range of 1,637–1,650 cm^{-1} and at 1,311 cm^{-1}, respectively [35]. Fig. 2I (f) illustrates the typical FTIR spectra of PAN. The spectra of PAN show a sharp band at 2,240 cm^{-1} for C≡N and a band at 1,074 cm^{-1} for C–N amide stretching [36,38]. The bands in the regions of 2,870–2,944, 1,450–1,460, 1,350–1,380, and 1,220–1,270 cm^{-1} are assigned to CH, CH_2, and CH_3 vibrations, respectively [39]. The FTIR spectra for the CS/PAN blends (Fig. 2I (b)–(e)) showed no observable change in the positions of the characteristic bands of CS (at 3,500–3,450 cm^{-1} for NH_2 and –OH stretching vibration, and at 1,640–1,650 cm^{-1} for amide I) and PAN (at 2,240 cm^{-1} for C≡N and at 1,074 cm^{-1} for C–N amide stretching). However, the intensities of these characteristic bands were observed to decrease and increase, when the blending ratio of the CS and PAN was changed in the blends. This behavior could be attributed to the overcrowding of the absorption bands of the CS by PAN and vice versa. The no observable change in the positions of the characteristics bands of CS and PAN indicates that there were no true chemical interactions between the two polymers. Fig. 2II(a) and (b) shows the FTIR spectra for CS and sIPN hydrogel films. An increase in the intensities of the bands at 1,024 and 1,384 cm^{-1} was observed for sIPN (Fig. 2II(b)), indicating C–O bond, which is typical of the ECH cross-linking of CS [40].

3.3. Degree of swelling

Fig. 3(a) and (b) illustrates the % degree of swelling of CS/PAN blends (C8/P2, C6/P4, C4/P6, and C2/P8) and sIPN (a-sIPN, b-sIPN, c-sIPN, and d-sIPN) hydrogel films as function of time. The % degree of swelling for all the CS/PANs increased sharply until~300 min and reached equilibrium at ~480 min. The highest % degree of swelling (~2,400%) was

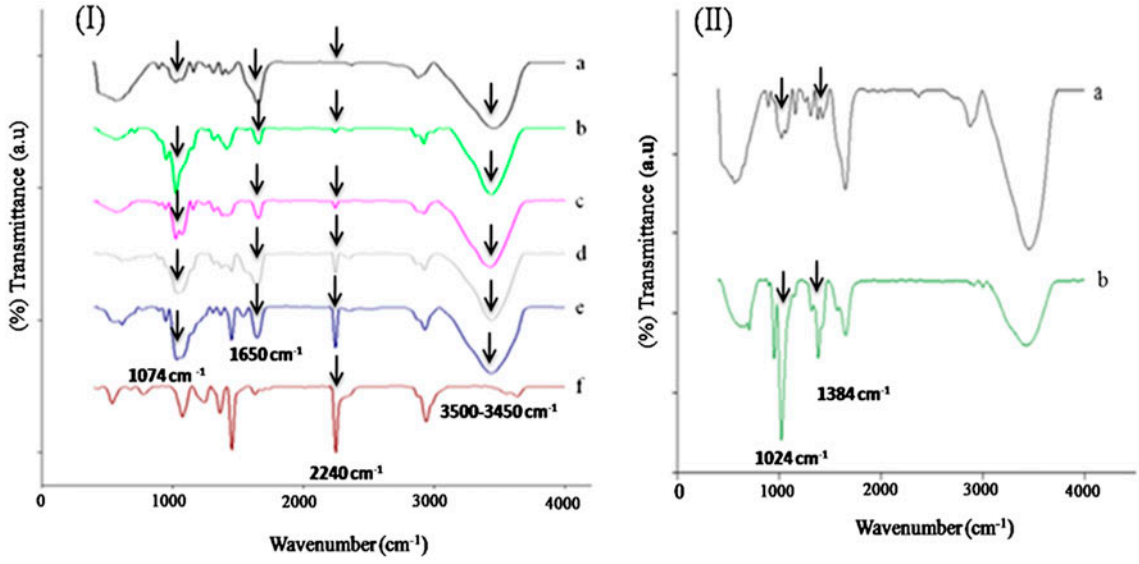

Fig. 2. FTIR spectra: I (a) CS, (b) C8/P2, (c) C6/P4, (d) C4/P6, (e) C2/P8, and (f) PAN; and II (a) CS and (b) c-sIPN.

recorded for C8/P2 blend film. However, as the quantity of PAN was increased in the blend, the % degree of swelling decreased in the order: C6/P4 (435%) > C4/P6 (126%) > C2/P8 (20%). The decrease in the % degree of swelling of the blend with an increase in the PAN amount could be attributed to the formation of hydrogen bonds between CS and PAN. These hydrogen bonds have not only resulted in the formation of compact structure and but also increased the hydrophobicity of blends [41]. The % degree of swelling of the blend sample (C8/P2) decreased to ~245% when it was converted to sIPN (c-sIPN (Fig. 3(b)). A similar decrease in the % degree of swelling is also reported by Tiwary and Rana [42,43].

However, the % degree swelling of the various sIPNs tabulated in Table 1 shows an increase in swelling with an increase in the cross-linker (ECH) concentration until 0.03 Mol L^{-1} (c-sIPN), beyond which it decreased. The order of the % degree of swelling for sIPN was: a-sIPN (~200) < b-sIPN (~215) < d-sIPN (~225) and c-sIPN (~245). This increase could be attributed to the availability of active site in sIPN until the critical concentration of cross-linker (0.03 Mol L^{-1}). Whereas the decrease in the % degree of swelling with an increase in the cross-linker (>0.03 Mol L^{-1}) might be attributed to phase separation and subsequent heterogeneous network structure formation [44].

3.4. Stability study

Fig. 4 shows the % degree of stability of CS/PAN blend and sIPN hydrogel films (calculated with Eq. (2)) in an aqueous solution, at pH 7 and up to 96 h. The CS/PAN blend films (Fig. 4(a)) with more than 50% PAN content (C4/P6 and C2/P8) attained a good % degree of stability, whereas when the % of PAN content is decreased to less than 50% (C8/P2, C6/P4), the % degree of stability of the films sharply dropped and became constant at ~70 h. The sharp decrease in the % degree of stability could be attributed to the more hydrophilicity and susceptibility of the CS to degradation [45]. To overcome this issue, CS in the blend sample (C8/P2) was cross-linked with ECH (Table 1). The resulting sIPN hydrogel films (Fig. 4(b)) showed an enhanced degree of stability (78, 82, 83, and 88% for a-sIPN, b-sIPN, c-sIPN, and d-sIPN, respectively). The increase in the % degree of stability was resulted from the increased cross-linking of CS chains [46] with ECH.

3.5. State of water study

Three types of water i.e. (unbound ((W_{UB}) freezing), intermediate ((W_I) freezing bound), and bound ((W_B) nonfreezing) are reported for hydrogel in the literature [5,35]. Unbound water does not form any bonds with polymer molecules, whereas intermediate water shows week interactions and bound water forms hydrogen bonds with polymer molecules. The water which forms hydrogen bonds with polymer cannot be freezed and W_{UB} therefore represents both W_B and intermediate. Table 2 shows the states of water (calculated using Eqs. (3)–(5)) for the CS/PAN blends and sIPN hydrogel films. The W_T and W_{UB} contents

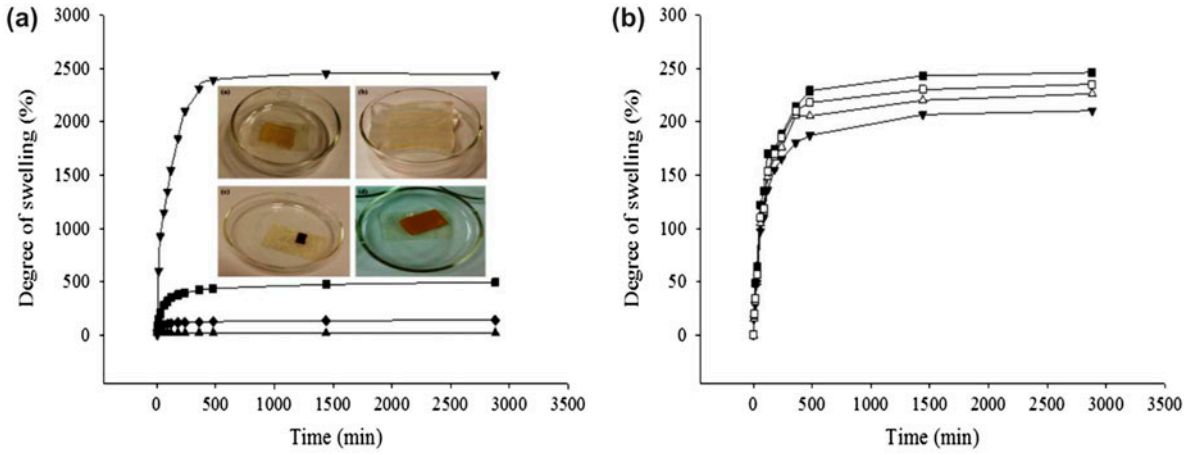

Fig. 3. Kinetic data of the % degree of swelling: (a) CS/PAN blend hydrogels: (▼) C8/P2, (■) C6/P4, (♦) C4/P6, and (▲) C2/P8; and (b) sIPN hydrogels: (▼) a-sIPN, (Δ) b-sIPN, (■) c-sIPN, and (□) d-sIPN. The inset digital images shows: (a) unswollen and (b) swollen C8/P2 blend films, and (c) unswollen and (d) swollen c-sIPN hydrogel.

were higher for CS/PAN C8/P2 blend films. The remaining films (C6/P4, C4/P6, and C2/P8) recorded almost constant W_B, and decreased W_T and W_{UB} contents. This behavior of the blend films could be attributed to the nearly a constant contact area between water and hydrogel, and the increased content of PAN in the hydrogel films. sIPN hydrogel films showed maximum W_T and W_{UB} for c-sIPN and d-sIPN hydrogel films. The remaining sIPN hydrogel films (a-sIPN and b-sIPN) showed less content of W_T and W_{UB} water. All the sIPN hydrogel films showed increased W_B, and decreased W_T and W_{UB} compared to their counterpart C8/P2 blend film. The increase in W_B could be attributed to the increase in contact area between the water and sIPN hydrogel films due to the induction of new water-contacting point during cross-linking. The water content followed similar pattern as was reported for equilibrium swelling (Fig. 3(a) and (b)).

3.6. Freeze dried hydrogel films morphology

Fig. 5(I) and (II) shows the schematic for the freeze drying process and FESEM micrographs (with the inset digital images) of freeze-dried blends and sIPN films. The surfaces of the films (Fig. 5II(a–e)) were

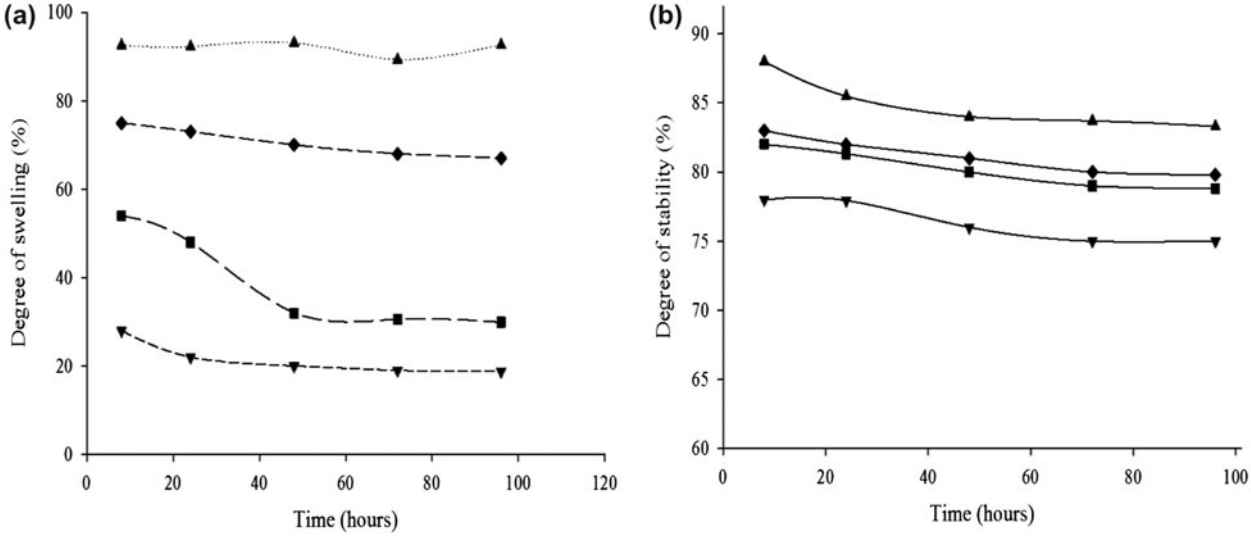

Fig. 4. % degree of stability at different time intervals: (a) CS/PAN blend: (▼) C8/P2, (■) C6/P4, (♦) C4/P6, and (▲) C2/P8; and (b) sIPN hydrogels: (▼) a-sIPN, (■) b-sIPN, (♦) c-sIPN, and (▲) d-sIPN.

Table 2
The amount and states of water in the hydrogel films using Eqs. (3)–(5)

Sample	W_T (%)	W_B (%)	W_{UB} (%)
CS/PAN blend films			
C8/P2	94.2	41.9	52.3
C6/P4	81.0	44.0	44.3
C4/P6	70.2	46.9	24.6
C2/P8	64.2	49.5	15.9
IPN hydrogel film			
a-sIPN	67.4	53.6	14.0
b-sIPN	69.1	53.1	16.0
c-sIPN	73.2	51.9	21.1
d-sIPN	72.1	53.8	18.2

homogeneous and closed with no porosity. The homogeneity of the surfaces could be attributed to the good miscibility of CS and PAN [5]. The cross-sectional surface of the film (Fig. 5(a′)) showed a highly porous structure for C8/C2 while homogeneous and closed structures for C4/P6 and C2/P8 films (Fig. 5(c′) and (d′)). sIPN film, however, showed much reduced porosity (Fig. 5(e′)). The difference in porosity for blend and sIPN films could be attributed to the difference in the % degree of swelling [5]. Similar relationship of the porosity and degree of swelling is also reported by Pulat and Özgündüz [20]. The porous structure of the films might form a potential adsorbent for sorption of dyes from the wastewater. However, the stability of the adsorbent films is also very important.

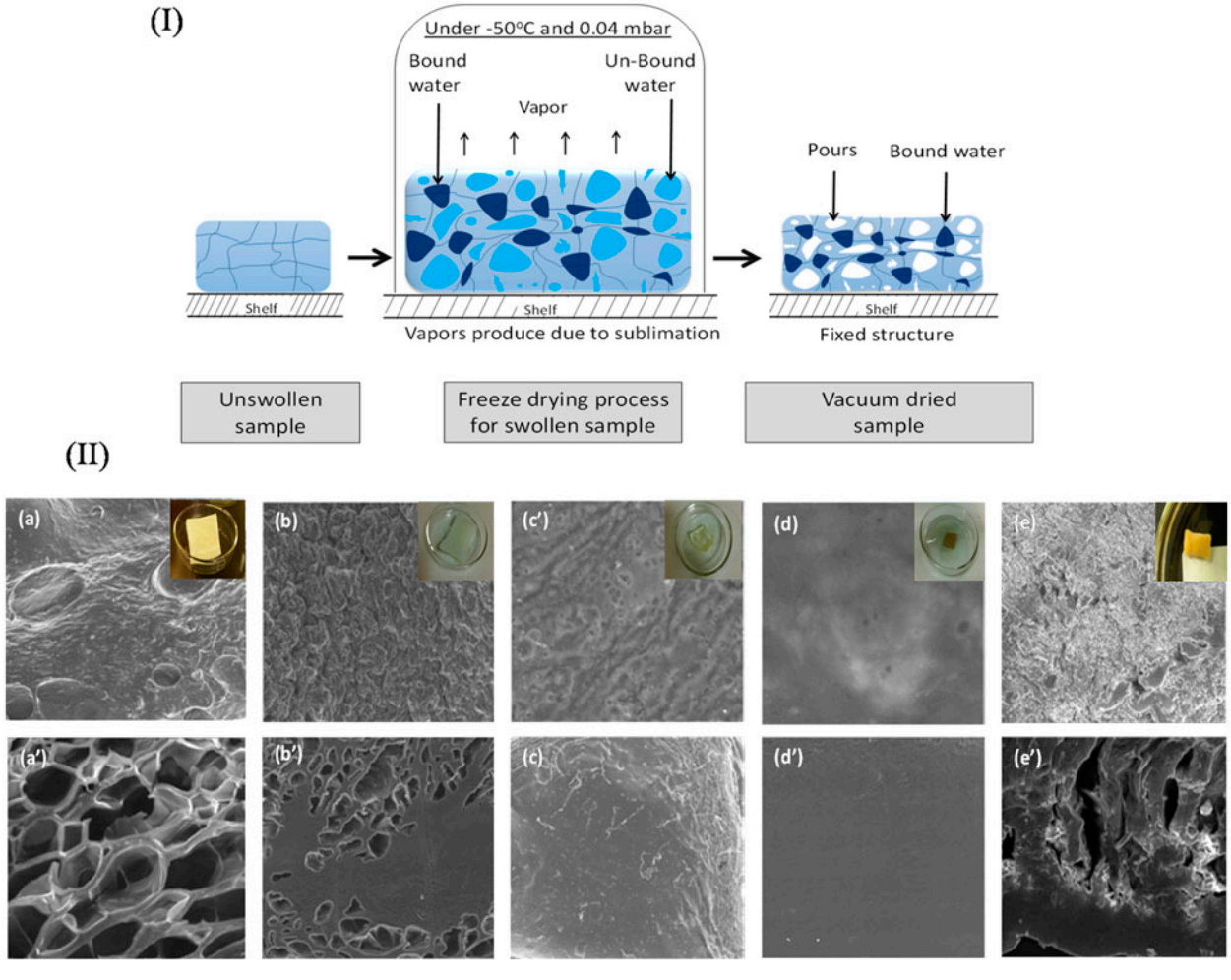

Fig. 5. (I) Schematic of the hydrogel freeze drying process and (II) FESEM micrographs of the surface of the freeze-dried hydrogels; (a) C8/P2, (b) C6/P4, (c) C4/P6, (d) C2/P8, and (e) c-sIPN and cross section; (a′) C8/P2, (b′) C6/P4, (c′) C4/P6, (d′) C2/P8, and (e′) c-sIPN.

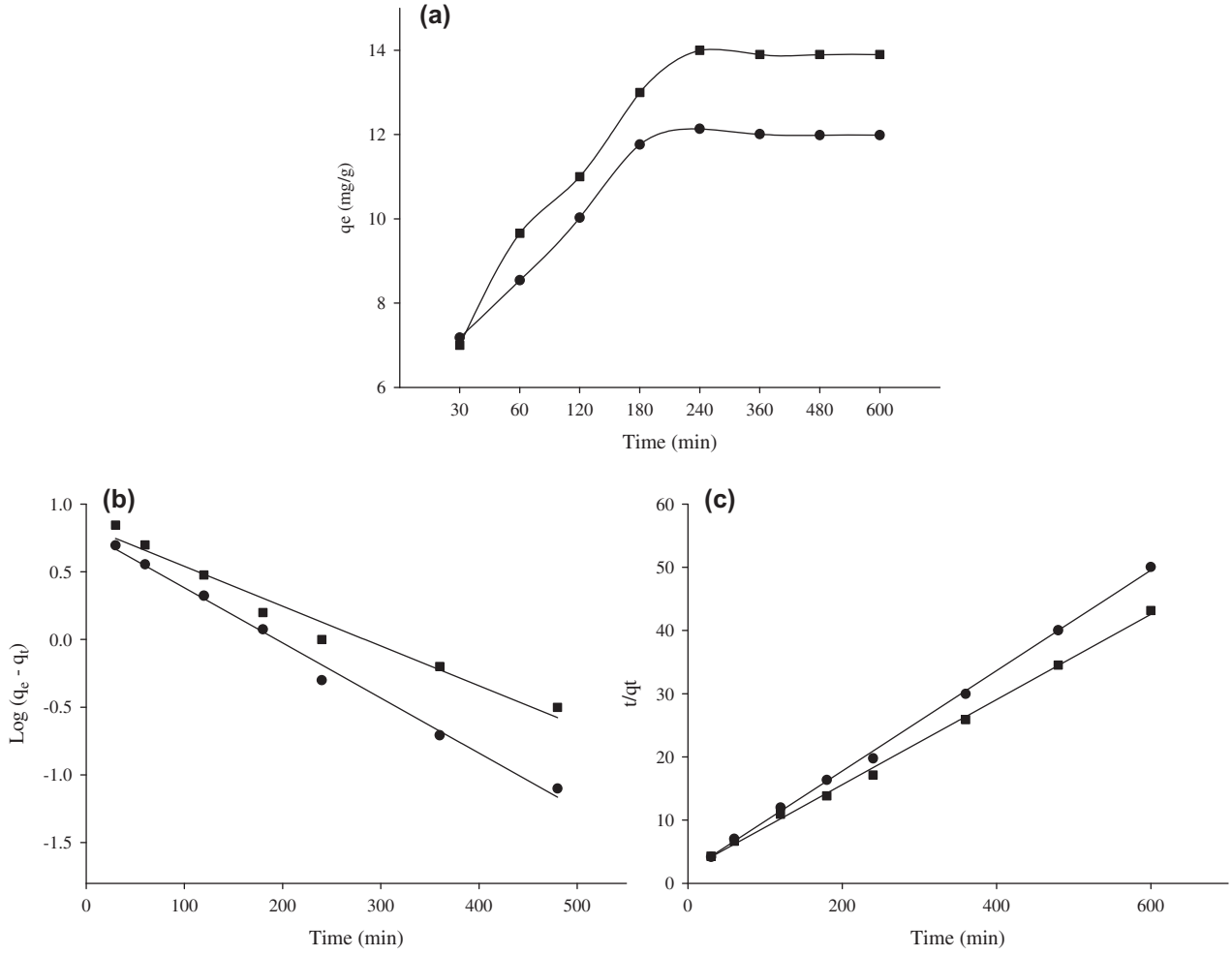

Fig. 6. (a) Adsorption of RB as a function of time, (b) pseudo-first-order, and (c) pseudo-second-order adsorption kinetics of RB dye onto (●) C8/P2 and (■) c-sIPN hydrogel films.

3.7. Adsorption study

3.7.1. Kinetic study

Fig. 6(a)–(c) shows the adsorption kinetics of RB onto CS/PAN blend (C8/P2) and sIPN (c-sIPN) hydrogel films from 100 ppm synthetic solution. The amount of dye adsorption was found to increase sharply until ~200 min and leveled off at ~240 min. The shapes of the curves illustrated that the binding of the dye to active sites on the adsorbent rapidly increased until ~200 min and saturate the surface of the adsorbent homogeneously at ~240 min. At the saturation point, there is equilibrium between adsorption and desorption of dyes. Furthermore, c-sIPN showed enhanced adsorption for RB comparing with C8/P2 hydrogel film. These results suggest that c-sIPN has more affinity to RB. The increase in the dyes' adsorption for c-sIPN could be attributed to the increased ECH cross-linking, which has resulted in an increase in the number of active sites onto sIPN hydrogel films. This observation is coherent with the increase in W_B water content for c-sIPN as shown in Table 2. To get a further insight and understanding of the process of dye adsorption onto the selected hydrogels, the data obtained from the kinetic study were further analyzed by pseudo-first-order (Eq. (7)) and pseudo-second-order kinetic (Eq. (8)) models. The pseudo-first-order kinetic model is based on the approximation that the adsorption rate relates to the number of the unoccupied adsorptive sites [46,47]. The pseudo-second-order kinetic model is based on the notion that the adsorption should be related to the squared product of the difference between the number of the equilibrium adsorptive sites available on an adsorbent and that of the occupied sites [31,48].

Table 3
Comparison of correlation coefficients, calculated, and experimental "q" values for the pseudo-first- and second-order kinetics models

	Adsorbent	q_{exp} (mg/g)	$K_1 \times 10^{-3}$ (min)	q_e (mg/g)	r^2
Rhodamine B	Pseudo-first-order				
	C8/P2	11	3.9	2.6	0.995
	c-sIPN	14	2.9	6.8	0.968
	Pseudo-second-order				
		q_{exp} (mg/g)	$K_2 \times 10^{-3}$(min)	q_e (mg/g)	r^2
	C8/P2	11	10.0	10.6	0.999
	c-sIPN	14	2.1	14.8	0.998

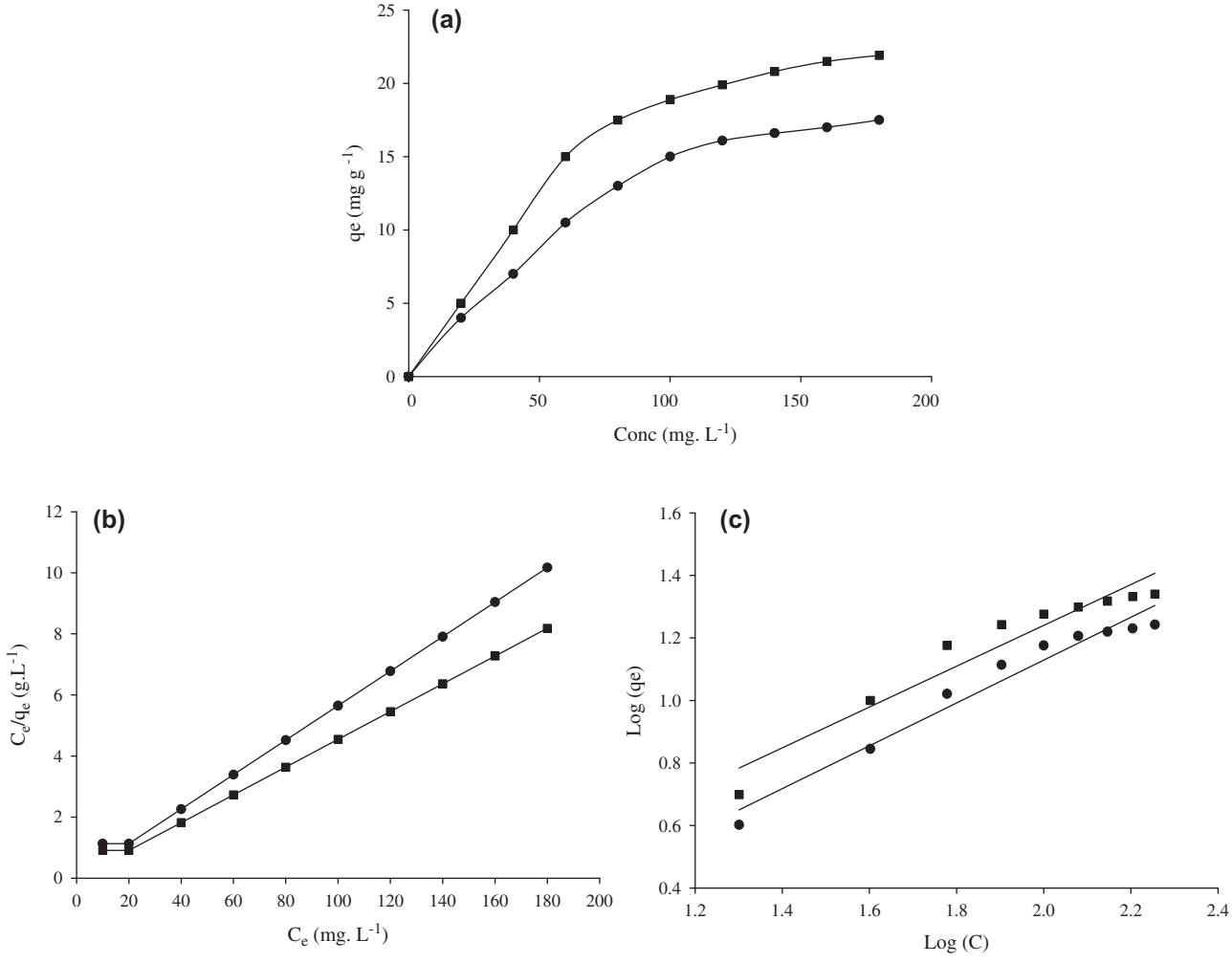

Fig. 7. (a) Adsorption of RB dye at different concentrations, (b) Langmuir, and (c) Freundlich isotherm for the adsorption of dyes onto (●) C8/P2 and (■) c-sIPN hydrogel films.

Table 4
Langmuir and Freundlich constants for the adsorption of dyes onto hydrogel films

	Langmuir			Freundlich		
Hydrogel samples	q_{max}	K_L	r^2	K_F	n	r^2
C8/P2	16	0.25	0.998	2.92	1.30	0.980
c-sIPN	21.9	0.30	0.999	1.16	1.53	0.930

$$\log(q_e - q_t) = \log(q_e) - \frac{K_1}{2.303}t \quad (7)$$

$$\frac{t}{q_t} = \frac{1}{K_2 q_e^2} + \frac{1}{q_e}t \quad (8)$$

where q_e and K_1, and q_e and K_2 can be obtained by the intercept and slope of the plots $\log(q_e - q_t)$ vs. t, and t/q_t vs. t, respectively.

Fig. 6(b) and (c), and Table 3 show the correlation coefficients of the adsorption data for pseudo-first-order and pseudo-second-order kinetic models. The best fit model was determined from the linear correlation coefficient values. Good fitting of the data was observed with the pseudo-second-order kinetic modal compared to the pseudo-first-order kinetic model. Furthermore, the q_e values obtained from the pseudo-second-order kinetic model for RB were much closer to the experimental q_{exp} values. These results suggested that the adsorption of RB follows pseudo-second-order kinetic model, which further suggests that the dye molecules are adsorbed onto two sorption sites on the surface.

3.7.2. Adsorption isotherm

Fig. 7(a) shows the equilibrium adsorption of RB onto the CS/PAN (C8/P2) and c-sIPN hydrogel films as a function of concentration (mg L^{-1}). Initially, the adsorption of the dyes increased rapidly, however as the concentration of RB was increased, adsorption gradually decreased. The gradual decrease in the adsorption of RB is an indication of the attainment of the equilibrium by the films. Fig. 7(b) and (c) shows that the adsorption data fitted to Langmuir and Freundlich equations. The Langmuir theory suggests that adsorption takes place at specific homogeneous sites within the adsorbent and once a dye occupied a reaction site (monolayer formation), then no further adsorption can occur at that location (chemical adsorption). Whereas, the Freundlich theory assumes that there occurs some non-chemical or physical adsorption, which forms more than one layer [49,50]. The value of correlation coefficient (r^2) for Langmuir varied from 0.997 to 0.999 and for Freundlich from 0.930 to 0.980. The increased values of the correlation coefficient in case of Langmuir suggested the formation of monolayer. The formation of monolayer further confirms the results of pseudo-second-order kinetic model. Table 4 shows the values of q_m and K_L for Langmuir isotherm, and n and K_F for Freundlich isotherm, which were calculated from the slope and

Table 5
Comparative data of dye adsorption on various adsorbents

Hydrogel	Dye	Conditions	Amount adsorbed (mg/g)	Refs.
Poly(AM-co-AA)	Methyl violet	pH 7 Temperature 25°C	5.81	[51]
Poly(AM-co-AA)	Methyl violet	pH 7 Temperature 25°C	5.73	[51]
PAMHEMA/CMC IPN	Basic fuschin	pH 7 Temperature 25°C	5.96	[52]
Coir pith	Methylene blue	pH 6.9 Temperature 25°C	5.87	[53]
Polyacrylamide/chitosan sIPN	Direct blue 1	pH 5.5 Temperature 25°C	2.80	[54]
Polyacrylamide/chitosan sIPN	Methylene blue	pH 5.5 Temperature 25°C	0.39	[55]
CS/PAN blend	Rhodamine B	pH 7 Temperature 25°C	16.00	Present study
c-sIPN	Rhodamine B	pH 7 Temperature 25°C	21.90	Present study

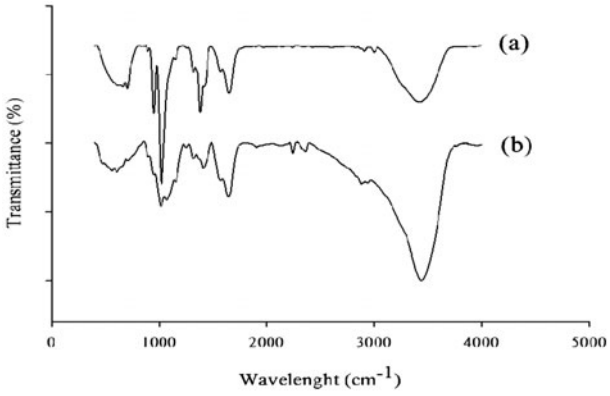

Fig. 8. FTIR spectra of c-sIPN (a) before and (b) after the adsorption of RB.

intercept of the plots. The q_{max} value for c-sIPN was much higher compared to C8/P2 blend film. The increased q_{max} value for c-sIPN could be attributed to the increase in the number of active sites and higher stability in aqueous medium. Tabulated comparison for the present work with an already reported work is given in Table 5, which shows that the adsorption of dyes preferred pH 7.0.

3.7.3. FTIR study of sIPN after adsorption

Fig. 8 shows the FTIR spectra of c-sIPN before (a) and after adsorption (b). The amide I and amide III bands in the range of 1,637–1,650 cm^{-1} and at 1,311 cm^{-1}, respectively, are typical of chitosan [35]. The increased band intensities at 1,024 and 1,384 cm^{-1} for c-sIPN indicates the formation of C–O bond, which is the characteristic of the ECH cross-linking of CS [40]. In the RB adsorbed c-sIPN spectra, the complex bands of the RB did not appear in the adsorbed state [56]. The band positions of the c-sIPN did not change either, however, the band at 1,637-1,650 cm^{-1} (amide I) and 1,348 cm^{-1} (amide III), whereas the bands at 1,024 and 1,384 cm^{-1} shifted, became broad and reduced in intensities. The shift, broadness, and decrease in intensities of these bands could be related to the hydrogen bonds formation between c-sIPN and RB [57]. Hydrogen bond formation is well documented in the literature for functional materials (containing electronegative atoms such as oxygen (EN; 3.44), nitrogen (EN; 3.04), and sulfur EN; 2.58)). Strong polarization of the hydrogen occurs when an electronegative atom is involved in the bond. The polarized hydrogen forms an electrostatic bond with the electronegative atom of another molecule. From FTIR, it was obvious that the mode of interaction between the c-sIPN hydrogel film and RB was hydrogen bonding [57]. No evidence of the chemical bonding of the dye molecules with c-sIPN film was obtained, which could be attributed to the absence of the complex peaking of dyes in the adsorbed state.

4. Conclusion

The preparation of CS/PAN blend and sIPN hydrogels and their application to the adsorption of RB dye were focused in this study. The CS/PAN blend films were prepared by solution casting technique. CS in the blend was cross-linked with ECH to prepare sIPN. The cross-linking of CS in the blend was confirmed by FTIR. The FESEM micrographs showed no phase separation between CS and PAN for both blend and sIPN films. The blend (C8/P2) film showed a highest degree of swelling (2,400%), increased % W_{UB} (52%), and fair degree of aqueous stability (28%), whereas sIPN hydrogel exhibited a relatively low degree of swelling (245%), W_{UB} (21%), and a high degree of aqueous stability (85.5%). The adsorption kinetics was observed to follow pseudo-second-order equation and equilibrium adsorption obeyed the Langmuir isotherm equation. The q_{max} value for sIPN was much higher compared to C8/P2 film. Both kinetic and isotherm results indicated that the mechanism of adsorption is chemical. However, FTIR gave no evidence of chemical bond formation.

Acknowledgements

The authors would like to extend their sincere appreciation to the Deanship of Scientific Research at King Saud University for its funding for this research group project No. (RG-1435-078).

References

[1] E.M. Ahmed, Hydrogel: Preparation, characterization, and applications, J. Adv. Res. 6 (2015) 105–121.
[2] A.S. Hoffman, Hydrogels for biomedical applications, Adv. Drug Delivery Rev. 54 (2002) 3–12.
[3] P. Riccardo, Water-absorbent polymers: A patent survey, J. Macromol. Sci. Rev. Macromol. Chem. Phys. 34 (1994) 607–662.
[4] E. Mah, R. Ghosh, Thermo-responsive hydrogels for stimuli-responsive membranes, Processes 1 (2013) 238–262.
[5] S. Haider, S.Y. Park, S.H. Lee, Preparation, swelling and electro-mechano-chemical behaviors of a gelatin–chitosan blend membrane, Soft Matter 4 (2008) 485–492.
[6] S.J. Kim, S.G. Yoon, K.B. Lee, Y.D. Park, S.I. Kim, Electrical sensitive behavior of a polyelectrolyte complex composed of chitosan/hyaluronic acid, Solid State Ionics 164 (2003) 199–204.

[7] R. Yoshida, T. Okano, Stimuli-Responsive Hydrogels and Their Application to Functional Materials. Biomedical Applications of Hydrogels Handbook, Springer Science Business Media, LLC, New York, NY, 2010, pp. 19–43.
[8] N. Bhattarai, J. Gunn, M.M. Zhang, Chitosan-based hydrogels for controlled, localized drug delivery, Adv. Drug Delivery Rev. 62 (2010) 83–99.
[9] Superabsorbents, Website of the European Disposables and Nonwovens Association (EDANA), 2008. Available from: <http://www.edana.org> (accessed 12 November 2014).
[10] J.Z.-M. Mohammad, K. Kourosh, Superabsorbent polymer materials: A review, Iran. Polym. J. 17 (2008) 451–477.
[11] A. Singh, S.S. Narvi, P.K. Dutta, N.D. Pandey, External stimuli response on a novel chitosan hydrogel crosslinked with formaldehyde, Bull. Mater. Sci. 29 (2006) 233–238.
[12] A. Sannino, C. Demitri, M. Madaghiele, Biodegradable cellulose-based hydrogels: Design and applications, Materials 2 (2009) 353–373.
[13] E.H. Schacht, Polymer chemistry and hydrogel systems, J. Phys. Conf. Ser. 3 (2000) 22–28.
[14] M. Pulat, H. Eksi, U. Abbasoglu, Fluconazole release from hydrogels including acrylamide-acrylic acid-itaconic acid, and their microbiological interactions, J. Biomater. Sci. Polym. Ed. 19 (2008) 193–205.
[15] M. Pulat, M. Çetin, Pantoprazole-Na release from poly (acrylamide-co-crotonic acid) and poly (acrylic acid-co-crotonic acid) hydrogels, J. Bioact. Compat. Polym. 23 (2008) 3054–3318.
[16] H. Saito, A. Sakurai, M. Sakakibara, H. Saga, Preparation and properties of transparent cellulose hydrogels, J. Appl. Polym. Sci. 90 (2003) 3020–3025.
[17] M. Pulat, D. Asıl, Fluconazole release through semi-interpenetrating polymer network hydrogels based on chitosan, acrylic acid, and citraconic acid, J. Appl. Polym. Sci. 113 (2009) 2613–2619.
[18] M. Pulat, N. Tan, F. Onurdağ, Swelling dynamics of IPN hydrogels including acrylamide-acrylic acid-chitosan and evaluation of their potential for controlled release of piperacillin-tazobactam, J. Appl. Polym. Sci. 120 (2011) 441–450.
[19] M. Pulat, G.O. Akalın, N.D. Karahan, Lipase release through semi-interpenetrating polymer network hydrogels based on chitosan, acrylamide, and citraconic acid, Artif. Cells, Nanomed. Biotechnol. 42 (2014) 121–127.
[20] M. Pulat, H.İ. Özgündüz, Swelling behavior and morphological properties of semi-ipn hydrogels based on ionic and non-ionic componenets, Biomed. Mater. Eng. 24 (2014) 1725–1733.
[21] M. Dash, M. Ferri, F. Chiellini, Synthesis and characterization of semi-interpenetrating polymer network hydrogel based on chitosan and poly(methacryloylglycylglycine), Mater. Chem. Phys. 135 (2012) 1070–1076.
[22] A.A. Oladipo, M. Gazi, Enhanced removal of crystal violet by low cost alginate/acid activated bentonite composite beads: Optimization and modelling using non-linear regression technique, J. Water Process Eng. 2 (2014) 43–52.
[23] A.A. Oladipo, M. Gazi, Nickel removal from aqueous solutions by alginate-based composite beads: Central composite design and artificial neural network modeling, J. Water Process Eng. (2014), doi: 10.1016/j.jwpe.2014.12.002.
[24] S.A. Ong, L.N. Ho, Y.S. Wong, Comparison on biodegradation of anionic dye orange II and cationic dye methylene blue by immobilized microorganisms on spent granular activated carbon, Desalin. Water Treat. 54 (2015) 557–561.
[25] A. Öztürk, E. Malkoc, Cationic basic yellow 2 (BY2) adsorption onto manure ash: Surface properties and adsorption mechanism, Desalin. Water Treat. 54 (2015) 209–226.
[26] N. Wang, Y. Han, Y. Liu, T. Bai, H. Gao, P. Zhang, W. Wang, W. Liu, High-strength hydrogel as a reusable adsorbent of copper ions, J. Hazard. Mater. 213–214 (2012) 258–264.
[27] L.A. Reis, L.L. Chiu, Y. Liang, K. Hyunh, A. Momen, M. Radisic, A peptide-modified chitosan-collagen hydrogel for cardiac cell culture and delivery, Acta Biomater. 8 (2012) 1022–1036.
[28] Y.S. Jeon, J. Lei, J.-H. Kim, Dye adsorption characteristics of alginate/polyaspartate hydrogels, J. Ind. Eng. Chem. 14 (2008) 726–731.
[29] L. Aberkane-Mechebbek, S.F. Larbi-Youcef, M. Mahlous, Adsorption of dyes and metal ions by acrylamide-co-acrylic acid hydrogels synthesized by gamma radiation, Mater. Sci. Forum 609 (2009) 255–259.
[30] A.A. Oladipo, M. Gazi, Microwaves initiated synthesis of activated carbon-based composite hydrogel for simultaneous removal of copper(II) ions and direct red 80 dye: A multi-component adsorption system, J. Taiwan Inst. Chem. Eng. 47 (2015) 125–136.
[31] K.C. Gupta, M.N.V. Ravi Kumar, Preparation, characterization and release profiles of pH-sensitive chitosan beads, Polym. Int. 49 (2000) 141–146.
[32] M. Kumar, B.P. Tripathi, V.K. Shahi, Crosslinked chitosan/polyvinyl alcohol blend beads for removal and recovery of Cd(II) from wastewater, J. Hazard. Mater. 172 (2009) 1041–1048.
[33] F. Sebesta, J. John, A. Motl, K. Stamberg, Evaluation of Polyacrylonitrile (PAN) as a Binding Polymer for Absorbers used to Treat Liquid Radioactive Wastes; Technical Report in Sandia National Labs., SciTech Connect, Albuquerque, NM, 1995, pp. 1–46.
[34] M. Aijaz, S. Haider, F. Mubddal, Y. Al-Zeghayer, W. Masry, Fabrication of chitosan/polyacrylonitrile blend and semi-IPN hydrogel with epichlorohydrin, AIP Conf. Proceed., 1664.030006 (2015), doi: 1063/1.4918396.
[35] V.R. Patel, M.M. Amiji, Preparation and characterization of freeze-dried chitosan-poly (Ethylene Oxide) hydrogels for site-specification antibiotic delivery in the stomach, Pharm. Res. 13 (1996) 588–593.
[36] H. Huang, Y. Hu, J. Zhang, H. Sato, H. Zhang, I. Noda, Y. Ozaki, Miscibility and hydrogen-bonding interactions in biodegradable polymer blends of poly(3-hydroxybutyrate) and a partially hydrolyzed poly(vinyl alcohol), J. Phys. Chem. B 109 (2005) 19175–19183.
[37] S. Viswanathan, M.D. Dadmun, Miscible blends containing a liquid crystalline polymer via optimized hydrogen bonding: Correlation to theory, J. Polym. Sci. Part B Polym. Phys. 42 (2004) 1010–1022.

[38] S.J. Kim, S.R. Shin, Y.M. Lee, S.I. Kim, Swelling characterizations of chitosan and polyacrylonitrile semi-interpenetrating polymer network hydrogels, J. Appl. Polym. Sci. 87 (2003) 2011–2015.
[39] A.V. Korobeinyk, R.L.D. Whitby, S.V. Mikhalovsky, High temperature oxidative resistance of polyacrylonitrile-methylmethacrylate copolymer powder converting to a carbonized monolith, Eur. Polym. J. 48 (2012) 97–104.
[40] R.S. Vieira, M.M. Beppu, Interaction of natural and crosslinked chitosan membranes with Hg(II) ions, Colloids Surf., A 279 (2006) 196–207.
[41] N. Hameed, Q. Guo, T. Hanley, Y.-W. Mai, Hydrogen bonding interactions, crystallization, and surface hydrophobicity in nanostructured epoxy/block copolymer blends, J. Polym. Sci.: Part B: Polym. Phys. 48 (2010) 790–800.
[42] A.K. Tiwary, V. Rana, Cross-linked chitosan films: Effect of cross-linking density on swelling parameters, Pak. J. Pharm. Sci. 23 (2010) 443–448.
[43] L. Mengatto, M.G. Ferreyra, A. Rubiolo, I. Rintoul, J. Luna, Hydrophilic and hydrophobic interactions in cross-linked chitosan membranes, Mater. Chem. Phys. 139 (2013) 181–186.
[44] Z.E. Meybodi, M. Imani, M. Atai, Kinetics of dextran crosslinking by epichlorohydrin: A rheometry and equilibrium swelling study, Carbohydr. Polym. 92 (2013) 1792–1798.
[45] S. Haider, Y. Al-Zeghayer, W.A. Al-Masry, F.A.A. Ali, Fabrication of chitosan nanofibers membrane with improved stability and britility, Adv. Sci. Lett. 17 (2012) 217–223.
[46] F.M. Goycoolea, A. Heras, I. Aranaz, G. Galed, M.E.F. Vall, W.A. Monal, Effect of chemical crosslinking on the swelling and shrinking properties of thermal and pH-responsive chitosan hydrogels macromol, Bioscience 3 (2003) 612–619.
[47] S. Haider, F.F. Binagag, A. Haider, W.A. Al-Masry, Electrospun oxime-grafted-polyacrylonitrile nanofiber membrane and its application to the adsorption of dyes, J. Polym. Res. 21 (2014) 371.
[48] W.J. Weber, J.C. Morris, Kinetics of adsorption of carbon from solutions, J. Sanit. Eng. Div. Am. Soc. Civ. Eng. 89 (1963) 31–59.
[49] K. Periasamy, C. Namasivayam, Process development for removal and recovery of cadmium from wastewater by a low-cost adsorbent: Adsorption rates and equilibrium studies, Ind. Eng. Chem. Res 33 (1994) 317–320.
[50] I.D. Mall, V.C. Srivastava, N.K. Agarwal, Removal of orange-G and methyl violet dyes by adsorption onto bagasse fly ash-kinetic study and equilibrium isotherm analyses, Dyes Pigm. 69 (2006) 210–223.
[51] D.S. Şolpan, Z.K. Kölge, Adsorption of methyl violet in aqueous solutions by poly(N-vinylpyrrolidone-co-methacrylic acid) hydrogels, Radiat. Phys. Chem. 75 (2006) 120–128.
[52] R. Bhattacharyya, S.K. Ray, Kinetic and equilibrium modeling for adsorption of textile dyes in aqueous solutions by carboxymethyl cellulose/poly (acryl amide-co-hydroxyethyl methacrylate) semi-interpenetrating network hydrogel, Polym. Eng. Sci. 53 (2013) 2439–2453.
[53] D. Kavitha, C. Namasivayam, Experimental and kinetic studies on methylene blue adsorption by coir pith carbon, Bioresour. Technol. 98 (2007) 14–21.
[54] E.S. Dragan, M.M. Perju, M.V. Dinu, Preparation and characterization of IPN composite hydrogels based on polyacrylamide and chitosan and their interaction with ionic dyes, Carbohydr. Polym. 88 (2012) 270–281.
[55] S. Kaur, S. Rani, R.K. Mahajan, Adsorption kinetics for the removal of hazardous dye congo red by biowaste materials as adsorbents, J. Chem. 2013 (2013) 1–12.
[56] H. Guolin, Y. Chuo, Z. Kai, S.H.I. Jeffrey, Adsorptive removal of copper ions from aqueous solution using cross-linked magnetic chitosan beads, Chin. J. Chem. Eng. 17 (2009) 960–966.
[57] S. Haider, F.F. Binagag, A. Haider, A. Mahmood, W.A. Al-Masry, M. Alhoshan, S.U.-D. Khan, Fabrication of the diethylenetriamine grafted polyacrylonitrile electrospun nanofibers membrane for the aqueous removal of cationic, Dyes Sci. Adv. Mater. 6 (2014) 309–318.